Desalination and Water Treatment
www.deswater.com
doi: 10.5004/dwt.2021.27897

244 (2021) 253–262
December

Response surface modeling of methylene blue dye removal from wastewater on natural oil shale

Maryem Rahmani[a], Boutaina Regraguy[a], Jamal Mabrouki[a], Ahmed Moufti[b,c], Mohamadine El'Mrabet[d], Abdelmalek Dahchour[d], Souad El Hajjaji[a,*]

[a]*Laboratory of Spectroscopy, Molecular Modeling, Materials, Nanomaterial's, Water and Environment (CERNE2D) Mohammed V University in Rabat, Faculty of Science, AV Ibn Battouta, BP1014, Agdal, Rabat, Morocco, emails: souad.elhajjaji@fsr.um5.ac.ma (S. El Hajjaji), rahmamnimeryem90@gmail.com (M. Rahmani), boutaina.reg21@gmail.com (B. Regraguy), jamalmabrouki@gmail.com (J. Mabrouki)*
[b]*Laboratoire des Sciences des Matériaux, des Milieux et de la Modélisation (LS3M), FPK, University Hassan 1, BP.145, 25000 Khouribga, Morocco, email: amoufti@gmail.com*
[c]*Regional Center for Careers in Education and Training, Casablanca-Settat, Morocco*
[d]*Department of Fundamental and Applied Sciences, Hassan II Agronomic and Veterinary Institute, BP 62002 Rabat-Institute 10000, Morocco, emails: mrabet2222@gmail.com (M. El'Mrabet), abdel_dahchour@yahoo.fr (A. Dahchour)*

Received 10 June 2021; Accepted 20 October 2021

ABSTRACT

In this work, the natural oil shale (NOS) performance was explored for removing methylene blue as textile pollutant. The adsorbent was characterized using X-ray fluorescence (XRF), X-ray diffraction (XRD), and scanning electron microscope (SEM). Further, the response surface methodology (RSM) was investigated to optimize the factors influencing the adsorption of MB onto NOS, using central composite design (CCD). The effect of the experimental parameters on adsorption yield, initial concentration of MB, mass of adsorbent, granulometry and pH, was studied using the response surface methodology (RSM). The obtained results show that the high MB adsorption rate (R% = 98%) is in a basic pH (pH = 12). The analyzes performed, based on residue and analysis of variance (ANOVA), confirmed that NOS had a high efficiency adsorbent capacity and that the chosen model is valid.

Keywords: Adsorption; Dyes; Methylene blue; Natural oil shale; Response surface methodology; Central composite design

1. Introduction

The textile industry effluents are strongly contaminated by dyes and has a huge impact on the aqueous environment [1,2]. A large volume of effluent contaminated by dyes is discharged, and 10%–15% of the used dye is lost in wastewater which damages the aesthetic nature of water, reduces the light penetration through the water's surface and the photosynthetic activity of aquatic organisms [1]. The fact that dyes are not easily biodegradable under aerobic conditions, due to the complexity of their chemical structure and the presence of aromatic rings, implies that the effluents require specific treatments [3,4]. Waste dyes can have severe environmental effects due to their toxicity, that human health and environment can be negatively impacted, [5]. The wastewater treatment remains a major challenge, especially for developing countries that do not yet have all the same opportunities to integrate the concepts of sustainable water management to protect its quality [3]. Hence, it is necessary to find the process

* Corresponding author.

of converting wastewater to be discharged back into the environment. Thus, the purpose of wastewater treatment is to speed up the natural processes by which water is purified [6]. Among the many techniques for treating Wastewater from dyestuff production is adsorption on natural materials such as oil shale, which has proven a great performance in the elimination of different pollutants [7] by the presence of the clay part in its composition [7–9].

To scientifically study the elimination of dyes by adsorption process, it is important to determine optimum conditions. This study is performed by the response surface methodology (RSM). The advantage of using this approach is that, it allows to control all the parameters influencing the study by a polynomial model, thus providing precision [10,11].

The aim of this work is to determine the effect of parameters, initial concentration of MB, pH, mass, and granulometry of adsorbent, and the interaction between factors, on MB adsorption onto natural oil shale (NOS). The second step is then the determination of the optimum conditions by the central composite design (CCD) and the validation of the chosen model.

2. Materials and methods

2.1. Preparation and characterization of the adsorbent

2.1.1. Materials

The MB chosen for this study was a synthetic dye obtained from "Fur di Microskopie" (Germany), its chemical structure is $C_{16}H_{18}ClN_3S$, with a molecular weight of 319.85 g/mol, its maximum wavelength is 664 nm, and it has a cationic character (Fig. 1).

2.1.2. Preparation of the adsorbent

The adsorbent used was NOS from Sekhirat city in Morocco; it has been milled and sieved to three granulometry: 30, 75, and 150 μm. It was in the form of a mixture of organic matter that comes from plants and microorganisms, and a mineral material (inorganic compounds) from the sediment deposition [8,12,13].

2.1.3. Characterization of the adsorbent

The chemical composition for the major oxides, some minor elements, and the loss on ignition of NOS were determined by X-ray fluorescence, using a PW1660 X-ray Spectrometer.

The mineralogical phases were analyzed by X-ray diffraction (XDR) using Siemens D5000 diffractometer with copper Kα1 diffraction line.

The morphological of NOS was investigated by scanning electron microscopy (SEM) (JEOL JFC-2300HR JEOL JSM-IT 100 scanning electron microscopy), attached with EDX unit (energy dispersive X-ray analyses), with accelerating voltage 30 kV.

The pH of the zero-charge point corresponds to the zero value of the surface potential [14]. For this investigation, 0.1 M NaCl was prepared, and its initial pH was adjusted between 2.0 and 12.0 by using NaOH or HCl. Then, 25 mL of 0.1 M NaCl was taken in the 100 mL flasks and 0.05 g of NOS was added to each solution. These flasks were kept for 24 h and the final pH of the solutions was measured by using a pH 210 Microprocessor pH meter. Graphs were plotted between pH final and pH initial [15].

2.2. Adsorption study

The experiments were carried out in a batch reactor presented in Fig. 2, at room temperature (25°C), and in the operating conditions as follow: initial concentration (from 20 to 40 ppm), mass of NOS (15, 30 mg), granulometry (30; 150 μm) and solution pH (4,12). A mass of NOS was added at 25 mL of dye solution in several initial concentration and pH. The solutions were stirred for 3 h, then, the suspensions were centrifuged at 3,000 rpm for 15 min. The residual concentration was determined using UV-Vis spectrophotometer at 664 nm.

The equilibrium adsorption capacity (Q_e) and the removal efficiency (R%) of the MB adsorbed on the NOS are calculated according to Eqs. (1) and (2).

$$Q_e = \frac{(C_0 - C_e) \times m}{V} \tag{1}$$

$$R(\%) = \frac{(C_0 - C_e)}{C_0} \times 100 \tag{2}$$

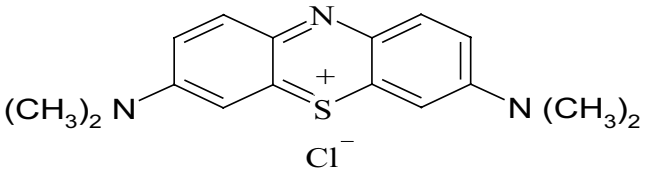

Fig. 1. Structure of methylene blue.

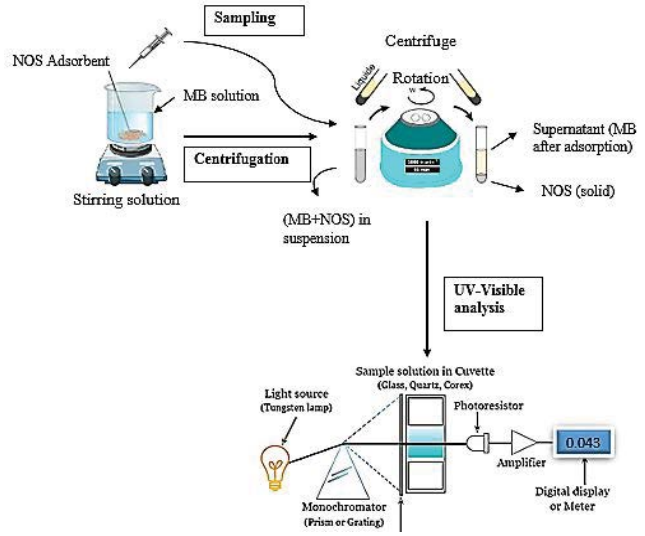

Fig. 2. Process flowsheet of the adsorption reactor.

where Q_e, is the amount of adsorbed dye per gram of adsorbents (mg/g) at equilibrium time, C_0 and C_e are respectively, the initial and equilibrium concentration of MB in solution ((g/L), V is the volume of the solution (L), and m is the mass of the adsorbent (g).

2.3. Design of experiment: response surface methodology

Adsorption process modeling was performed using the design of experiment (DOE), second degree. The effect of initial concentration of MB (X_1), mass of NOS (X_2), granulometry (X_3), pH (X_4), on the removal rate (%) Y, were analyzed individually using RSM. This present investigation is carried out by central composite design (CCD). The CCD comprised the usual 2^4 factorial design ordinarily denoted by n_f, 8 axial points symbolized by n_a, and 6 center points represented by n_c. The process factor settings were carefully selected to enable satisfactory coverage of the process variable values ordinarily encountered in the regions of practical interest [16,17]. Furthermore, the factor levels were coded using Eq. (3) [17]:

$$x_i = \frac{\left(f - M\right)}{S} \tag{3}$$

where "x_i" is the coded variable value, "f" represents the factor level, "M" represents the center, and "S" is half the deviation of the "low" factor level from the "high" level. The actual and coded values are summarized in Table 1. The total run given by CCD was calculated by Eq. (4) [16,18].

$$N = n_f + n_a + n_c = 2^n + 2n + n_c = 30 \tag{4}$$

Table 1 represents the experimental range of factors at two levels [high level (+1) and low level (–1)].

The experimental results were statistically analyzed by JMP software version 11, using the central composite design (CCD).

3. Results and discussion

3.1. Characterization of the adsorbent

3.1.1. XRF analysis

The results of the elementary analysis performed by the XRF are presented in Table 2. The NOS used in this study is rich in silica (52.56%) and alumina (23.12%). The mass loss after combustion corresponding to the ignition of loss (LOI) is 7.89.

Other oxides, such as K_2O, P_2O_5, and Na_2O, can be explained by presence of organic matter [19].

3.1.2. XRD analysis

The XRD analysis gave the same result obtained by the XRF. The SiO_2 presents most of the NOS composition. According to the XRD analyses, illustrated in Fig. 3, illite and kaolin clay minerals were identified as matrix clay in NOS [7].

3.1.3. SEM analysis

The elemental analysis and morphological structure of NOS are shown in Fig. 4. The NOS is presented in platelets form (Fig. 4a), which characterize clay, and aggregate's structure [7]. The EDX analysis confirms the results found by the FRX and DRX analysis, with the presence of the major elements: oxygen (44%) and silicon (20%) (Fig. 4b).

3.1.4. Determination of zero-point charge

The effect of pH may be explained by the zero-point charge (PZC) of the adsorbent (pHpzc of NOS is 7.98, Fig. 5), at which the adsorbent is neutral. The surface charge of the adsorbent is positive when solution pH is below pHpzc due to protonation of the functional groups [20]. An increase in pH above pHpzc will show a slight increase in adsorption if the dye species are still positively charged or neutral even though the surface of the adsorbent is negatively charged [20]. When both the surface charge of the adsorbent and dye species charge become negative, the adsorption will decrease significantly. Decrease in removal of MB at lower pH is apparently due to the higher concentrations of H^+ in the solution (Fig. 5), which compete with MB for the adsorption sites of NOS [21,22]. Generally, the positive charge of the adsorbent surface decreases with the increasing pH value, leading to the decrease in the

Table 1
Experimental range and levels of independent process factors

Variables (factors)	Code	Levels	
		–1	+1
Initial concentration, mg/L	X_1	20	40
Mass of NOS, mg	X_2	15	30
NOS granulometry, μm	X_3	30	150
pH	X_4	4	12

Table 2
Chemical composition of NOS by XRF

Composition	Value (%)
SiO_2	52.56
Al_2O_3	23.12
Fe_2O_3	7.81
CaO	1.83
MgO	0.87
SO_3	0.11
K_2O	4.15
TiO_2	0.98
MnO	0.13
P_2O_5	0.15
Na_2O	0.25
SrO	0.036
ZnO	0.02

repulsion between the adsorbent surface and MB, thus improving the adsorption capacity [23].

3.2. Statistical validation of CCD data

3.2.1. Experimental design

The design matrix is shown in Table 3. The axial runs represent the points which were located beyond the "low" (–1) and "high" (+1) process factor levels pertaining to the factorial segment of the experimental design matrix [17]. The values presented in Table 3, are given automatically by the chosen model (CCD).

In this study, the concentration of MB (X_1), mass of NOS (X_2), NOS granulometry (X_3), and pH (X_4) are used, the other parameters (temperature, stirring speed, etc.) were kept constant. The results of removal rate (%) are illustrated in Table 3.

The response, namely removal rate (R%), was individually correlated with the process factors using second-order models. Second-order or quadratic response surface design mathematical model is a polynomial as in Eq. (5) [17,24,25]:

$$Y = a_0 + a_1X_1 + a_2X_2 + a_3X_3 + a_4X_4 + a_{11}X_1^2 + a_{22}X_2^2 + a_{33}X_3^2 + a_{44}X_4^2 + a_{12}X_1X_2 + a_{13}X_1X_3 + a_{14}X_1X_4 + a_{24}X_2X_4 + a_{34}X_3X_4 + \varepsilon \quad (5)$$

where a_0 represents the average value of the response to the experiments. a_1, a_2, a_3, and a_4 are corresponding to concentration of MB, pH, mass, and granulometry of NOS. On the other hand, values a_{12}, a_{13}, a_{14}, a_{23}, a_{34}, and a_{24} correspond to interaction of first order, while a_{11}, a_{22}, a_{33}, and a_{44} are the interaction of the second order.

The model of removal% for MB onto NOS has been illustrated by the following regression formula [Eq. (6)]:

$$Y_{(NOS/BM)} = 65.91 - 12.4774X_1 + 8.3023X_2 - 7.267538X_3 + 6.6974X_4 + 4.6687X_1X_2 - 1.9487X_1X_3 + 5.0787X_2X_3 + 2.2575X_1X_4 - 4.3125X_2X_4 + 2.4675X_3X_4 + 3.7968X_1^2 + 2.6837X_2^2 - 0.2477X_3^2 + 1.3634X_4^2 \quad (6)$$

The second order equation for the polynomial model given by JMP 11 software, shows that the positive sign of the coefficients in the regression model (X_2, X_4, X_1X_2, X_2X_3, X_1X_4 X_3X_4, X_1^2, X_3^2, and X_4^2) account for a synergistic

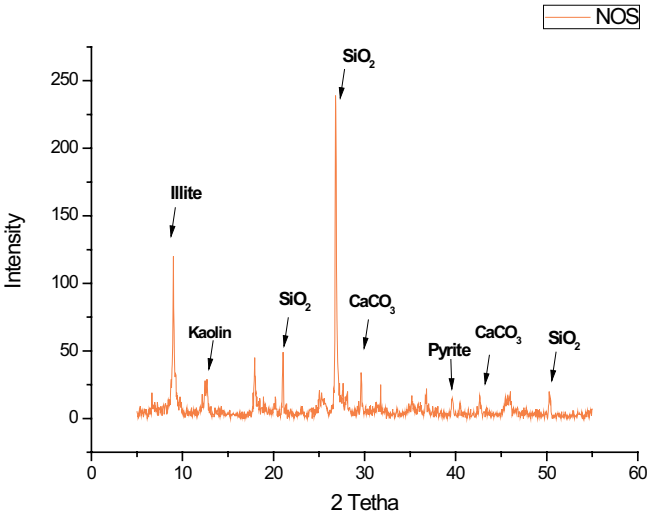

Fig. 3. X-ray patterns of NOS.

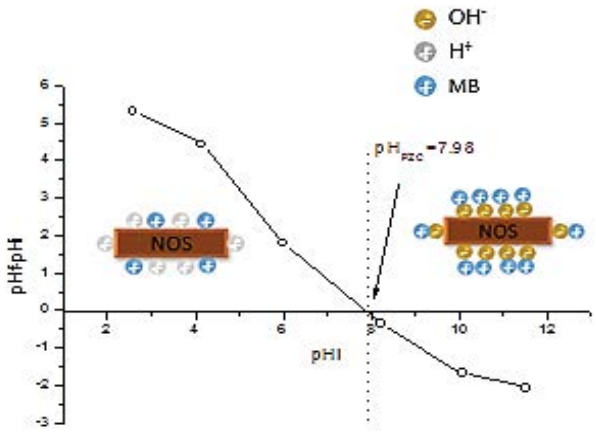

Fig. 5. Determination of surface charge of NOS by PZC.

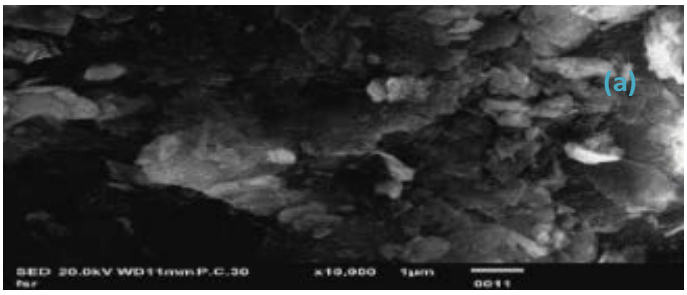

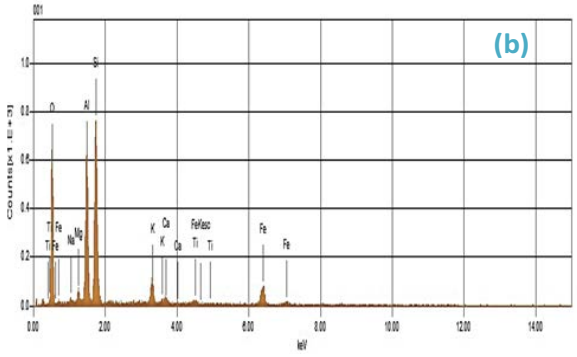

Fig. 4. SEM analysis: (a) scanning image of NOS and (b) EDX analysis.

Table 3
Experimental design matrix and obtained response given by the composite center design for adsorption study

Initial concentration of MB (X_1)	Mass of NOS (g) (X_2)	Granulometry (μm) (X_3)	pH (X_4)	Removal rate (%) (Y)
30	22.5	90	0.92	53.87
40 (+)	30 (+)	150 (+)	4 (–)	68.93
30	22.5	90	8	64.56
30	22.5	90	15.08	86.5
30	22.5	90	8	72.31
20 (–)	15 (–)	150	12 (+)	78.34
40	30	30 (–)	4	75.06
40	15	30	4	55.64
40	30	30	12	80.31
20	30	150	12	93.62
40	15	150	4	6.9
30	22.5	90	8	58.98
40	30	150	12	71.75
20	30	30	12	92.91
40	15	150	12	53.96
20	15	150	4	66.47
30	35.78	90	8	82.52
30	25	90	8	60.43
20	30	30	4	93.47
40	15	30	12	64.26
30	9.22	90	8	66.13
30	22.5	90	8	72.66
20	30	150	4	89.94
30	22.5	90	8	66.52
12.29	22.5	90	8	93.46
20	15	30	12	98.59
20	15	30	4	85.95
30	22.5	90	8	59.92
47.71	22.5	90	8	62.17

effect, whereas the negative sign reflects an antagonistic effect [26].

3.2.2. Analysis of variance

The analysis of variance (ANOVA) was performed to verify the validation of the quadratic model [27], it can be used to estimate whether the calculated effects are significant [28]. The best regression model is acquiring from the probabilistic value (p-value), thus, if it is less than 0.05 ($p < 0.05$), it indicates that the chosen model is good [29–31].

The statistical significance parameters used by quadratic models, are provided by coefficient of determination R-square (R^2), adjusted R-square (R^2adj.), root of mean square error, mean response, luck of fit, Prob. > F [32,27]. The values of these statistical models are listed in Table 4. The coefficient of determination (R^2 = 0.915828%) is sufficient. This value gives a good correlation between the experimental and predicted values of the adapted model [33]. The optimization of parameters was carried out by the desirability approach of RSM [34], this function allows us to obtain optimal adjustment that varies between 0 and 1. The value 0 is assigned when the factors are unacceptable (undesirable) response and 1 when the response represents the desired maximum performance for the significant factors [35].

3.2.3. Effect of the adsorption parameters

In this study, the most of parameters are statistically significant, where the p-value was less than 0.05, such us: initial concentration of MB (<0.0001), mass of NOS (0.0002), granulometry (0.0024), pH (0.0013), the interaction effect between: concentration and the mass of NOS (0.0315), the mass of NOS and granulometry (0.0211), the mass of NOS and pH (0.0443), these results are illustrated in Table 5.

According to these obtained results by the JMP software, the predictive equation in terms of significant parameters is shown in Eq. (7):

$$Y\left(\text{Removal rate \%}\right) = -12.4774\ X_1 + 8.3023\ X_2 - 7.2675\ X_3 + 6.6974X_4 + 4.66875X_1X_2 + 5.07875X_2X_3 - 4.3125X_2X_4 \quad (7)$$

Table 4
Analysis of variance and statistical parameters of central composite design

Source	Degrees of freedom	Sum of squares	Mean square	*F*-ratio
Model	14	8,489.0950	606.364	10.1032
Error	13	780.2191	60.017	Prob. > *F*
C. total	27	9,269.3141	–	<0.001
Statistical parameters				
R-square	*R*-square Adj.	Lack of fit	Root mean squared error	Mean of response
0.915828	0.825181	0.9820	7.747055	72.0075

Table 5
Estimate of coefficients by ANOVA analysis

Terms	Estimation	Standard error	*t*-ratio	Prob. > |*t*|
Constant	65.91	3.162722	20.84	<0.0001*
Initial concentration (20,40)	–12.47747	1.641596	–7.60	<0.0001*
Mass of NOS (15,30)	8.3023659	1.641596	5.06	0.0002*
Granulometry (30,150)	–7.2675	1.936764	3.75	0.0024*
pH (4,12)	6.6974514	1.641596	4.08	0.0013*
Initial concentration × Mass of NOS	4.66875	1.936764	2.41	0.0315*
Initial concentration × Granulometry	–1.94875	1.936764	–1.01	0.3327
Mass of NOS × Granulometry	5.07875	1.936764	2.62	0.0211*
Initial concentration × pH	2.2575	1.936764	1.17	0.2647
Mass of NOS × pH	–4.3125	1.936764	–2.23	0.0443*
Granulometry × pH	2.4675	1.936764	1.27	0.2250
Initial concentration × Initial concentration	3.7968078	2.017345	1.88	0.0824
Mass of NOS × Mass of NOS	2.6837579	2.017345	1.33	0.2063
Granulometry × Granulometry	–0.247722	3.595348	–0.07	0.9461
pH × pH	1.36340064	2.017345	0.68	0.5110

* presents the values of probability that is less than 0.005, that is, mean the significant effect.

This model shows that the initial concentration has a negative effect on the MB removal rate (%). When the mass of adsorbent increases, the removal rate decreases lightly then remains constant above 25 mg (Fig. 6), which explain that the cations of the dye can easily access to adsorption sites when the adsorbent mass is low, but, a large mass of adsorbent induces agglomeration and aggregation of particles, hence a reduction in the surface area and, consequently, a decrease in amount of adsorbate per unit mass of the adsorbent [36].

It is also noted that the response increases when the pH increases, the minimum adsorption observed at low pH (pH 4) (Fig. 6) may be due to the higher concentration and high mobility of H^+ ions which favored the adsorption of hydrogen ions over MB [37,38]. It is suggested that at lower pH values, the surface of the adsorbent is surrounded by hydronium ions (H^+), thereby preventing the dye ions from approaching the binding sites of the sorbent [38]. Similar observation has been noted by Azzaz et al. [39] for the MB removal onto chemical treatment of orange tree sawdust, it showed that more the surface of raw orange sawdust (ROS) is negatively charged, more it allows the attraction of positively charged MB at a pH 10.2. The desirability function obtained by this model is equal to 0.973 (Fig. 6).

3.2.3. Residue examination

The residue is defined the difference between the quantity measured and the quantity predicted by the model [40]. Residue analysis consists of comparing the residues as a function of the adsorbed experimental quantities. Fig. 7 presents the residue values for each experiment. It shows that the residue does not exceed the removal rate field. This residue is equally distributed in space which means that it has been accepted. Moreover, this illustrates that this model describes well the phenomenon studied [41].

3.3. Synergic effect of adsorption parameters

JMP software (version 11) was employed to present the three-dimensional (3D) response surface plots by varying two factors in function of the response, (Fig. 8). The first significant interactive effect between the mass of adsorbent and pH, provided in Fig. 8b, with *p*-value of 0.0443 proves the essential role of solution pH in elimination of MB onto NOS, therefore, the removal rate (%) of MB increase from 50% to 90% by increasing pH from 4 to 12 and increasing mass of NOS from 15 to 30 mg, which explain the difference of NOS surface charge in acidic and basic solution [38].

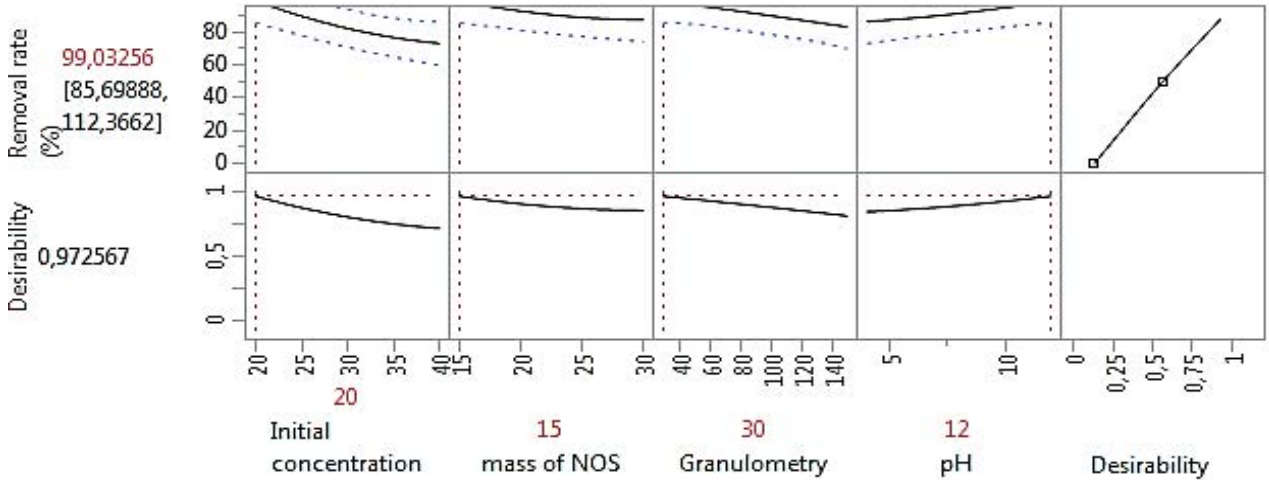

Fig. 6. Optimal conditions of MB removal and expected yield.

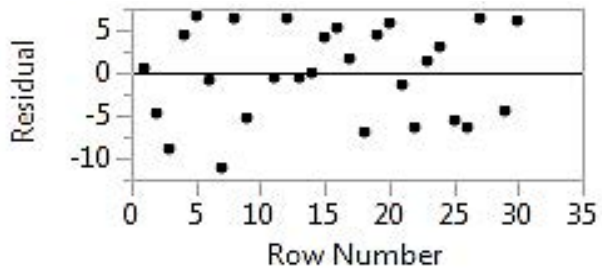

Fig. 7. Residue analysis for each experiment.

The second significant interactive effect can be observed between the mass of adsorbent and the concentration (0.0315) Fig. 8c, indicates that in the maximum level of the MB concentration (40 ppm) and with increasing the mass of NOS from 15 to 30 mg, the removal rate rises from 40% to 75%. The third significant interaction between mass of adsorbent and granulometry where the *p*-value = 0.0211, the removal rate decreased from 80% to 40% by increasing the granulometry of NOS from 30 to 150 μm, Fig. 8e, it can be explaining that the surface area of adsorbent, more it's high more the adsorption is efficient, on the other hand, at higher mass of adsorbent, strong driving force and large surface area would be available for exchangeable sites for dye ions [42].

4. Regeneration of NOS

The regeneration which is an interesting process in the adsorption phenomenon was carried out in this study to enhance the NOS and analyze its recoverability. The desorption study of MB was performed in the batch system by using HNO_3 (0.3 M) as the eluent to investigate potential regeneration of the adsorbent used. MB loaded NOS was dried for 24 h at 50°C. The results (Fig. 9) show an effectiveness of the NOS in the adsorption/desorption even after five cycles, hence, its advantage from the economic and environmental point of views. The increase efficiency of desorption from the first cycle to the five (from $Ads_{1st\ cycle}$ = 55.85%, $Des_{5th\ cycle}$ = 12.25%, to $Ads_{5th\ cycle}$ = 35.71%, $Des_{1st\ cycle}$ = 42.89%), with a maximal percentage in the third cycle ($Ads_{3rd\ cycle}$ = 11.89%, $Des_{3rd\ cycle}$ = 73.19%) can be explained by the weak bonds applied between the dye and the adsorbent due to the physisorption process [7].

5. Comparison with other adsorbents for the MB removal

To demonstrate the efficiency using NOS, of Sekhirat region, as a good adsorbent of MB elimination and other pollutants, indeed of its availability, and the recoverability of this adsorbent which can be used in textile industry with a high performance (*R*% = 98.59%), a comparison with other studies of MB removal is provided in Table 6. NOS of skhirate presents a good performance.

6. Conclusion

This present investigation shows that natural oil shale (NOS), as an inexpensive sorbent, has an important efficiency for removal textile dyes in aqueous solution especially MB (32.86 mg/g). The strong adsorption of cationic dyes is done at high pH. The characterization of adsorbent reveals that the matrix clay of oil shale consists of illite and kaolin, with a high percentage of SiO_2 and Al_2O_3. The modeling process of adsorption was statically optimized using flexible and reliable empirical models RSM. According to the statistical results, the effect of the initial concentration showed a negative impact on the removal efficiency of MB by NOS. However, all effects are significant on the elimination process of MB by adsorption on the NOS. The model envisaged for the optimal design has been well verified by the experimental data, with R^2 and R^2adj is 0.913 and 0.827, respectively. The maximum removal rate is obtained in the following optimum conditions: (X_1 = 20 mg/L) for the initial concentration, (X_2 = 15 mg) for the mass of NOS, (X_3 = 30 μm) for granulometry and (X_4 = 12) for pH. The MB dye is efficiently desorbed by nitric acid from adsorbed NOS. The reusability of the adsorbent used is found efficient after consecutive adsorption–desorption cycles.

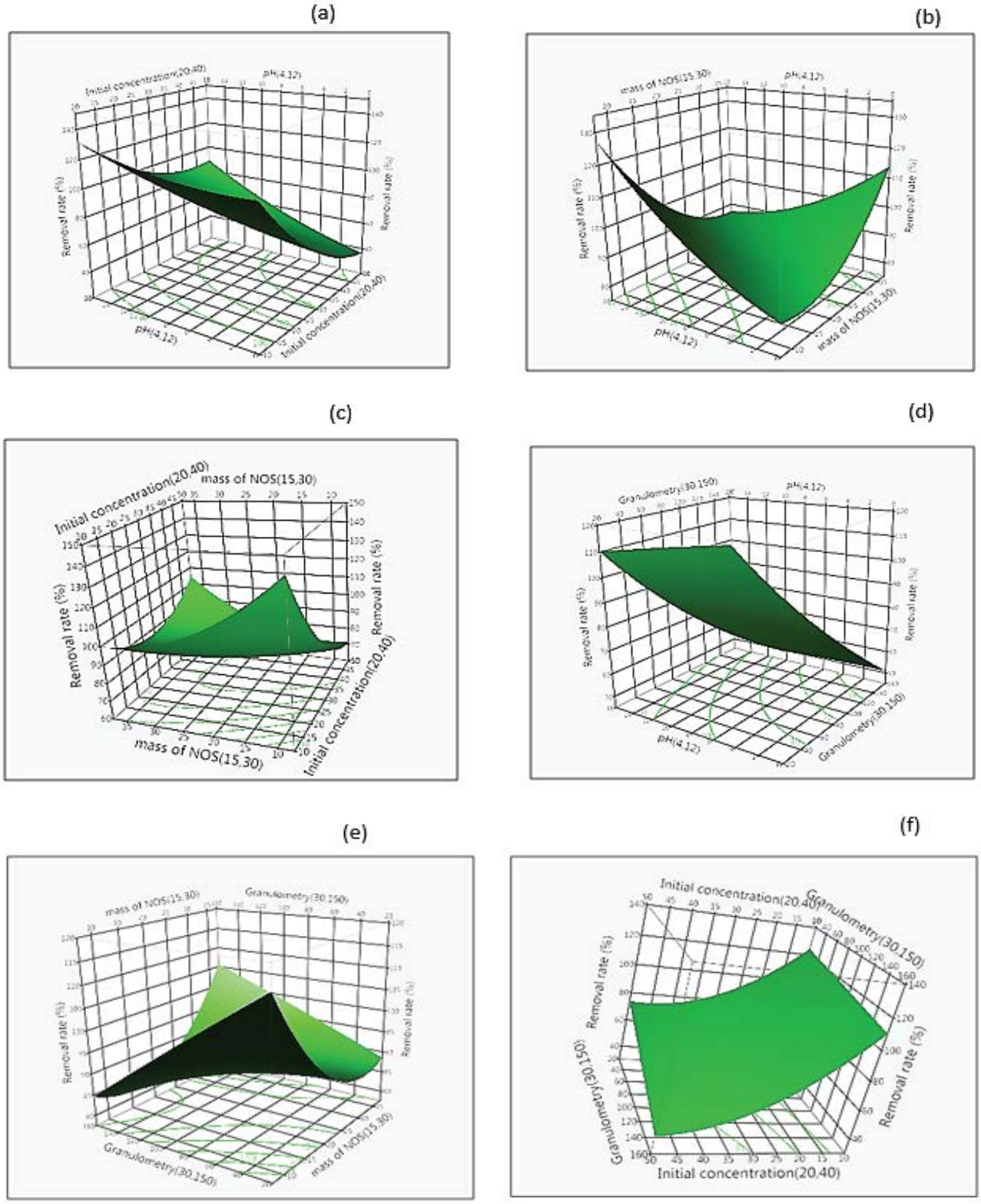

Fig. 8. Response surface model of removal rate (%) by four factors. Interaction between (a) initial concentration of MB and pH, (b) mass of NOS and pH, (c) mass of NOS and initial concentration, (d) pH and granulometry, (e) mass and granulometry of NOS, and (f) initial concentration and granulometry.

Table 6
Literature comparison of removal MB onto different adsorbents

Adsorbents	Sorption capacity (mg/g)	Reference
Homemade walnut carbon	3.74–4.74	[43]
Fe_3O_4/chitosan/graphene (FCG) nanocomposite	47.35	[44]
Raw oil shale (SSB)	50	[45]
oil shale decarbonated (SBD)	60	
Raw clay (AB)	75	
Decarbonated clay (AD)	115	
Raw orange sawdust	39.68	[46]
Clay loaded hydrochar	96.9 mg/g	[47]
Ruthenium nanoparticles on activated carbon (Ru/C)	9.25–48.40 mg/g	[48]
Natural oil shale (Tarfaya)	40.82	[49]
Natural oil shale (Skhirate)	32.86	This work

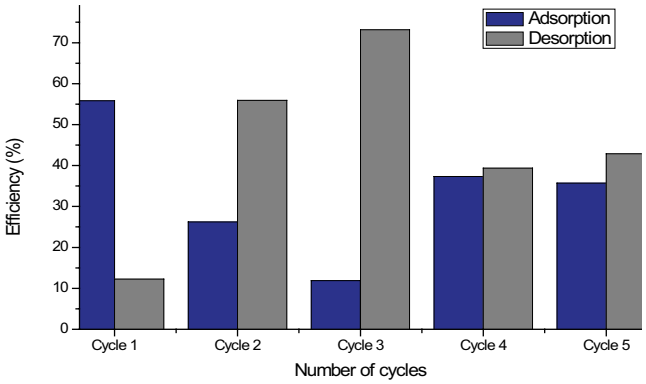

Fig. 9. Adsorption/desorption consecutive cycles of MB/NOS in batch system.

References

[1] H. Zollinger, Color Chemistry Synthesis, Properties and Application of Organic Dyes and Pigments, VCH, New York, NY, 1987.
[2] J. Mabrouki, G. Fattah, N. Al-Jadabi, Y. Abrouki, D. Dhiba, M. Azrour, S. El Hajjaji, Study, simulation, and modulation of solar thermal domestic hot water production systems, Model. Earth Syst. Environ., (2021) 1–10, doi: 10.1007/s40808-021-01200-w.
[3] I. Cabrita, B. Ruiz, A.S. Mestre, I.M. Fonseca, A.P. Carvalho, C.O. Ania, Removal of an analgesic using activated carbons prepared from urban and industrial residues, Chem. Eng. J., 163 (2010) 249–255.
[4] O.T. Ogunmodede, A.A. Ojo, E. Adewole, O.L. Adebayo, Adsorptive removal of anionic dye from aqueous solutions by mixture of Kaolin and Bentonite clay: characteristics, isotherm, kinetic and thermodynamic studies, IJEE J., 6 (2015) 147–153.
[5] I.J. Arslan, Treatability of a simulated disperse dye bath by ferrous iron coagulation, ozonation, and ferrous iron-catalyzed ozonation, J. Hazard. Mater., 85 (2001) 229–241.
[6] Y. El Mouzdahir, A. Elmchaouri, R. Mahboub, A. Gil, S.A. Korili, Equilibrium modeling for the adsorption of methylene blue from aqueous solutions on activated clay minerals, Desalination, 250 (2010) 335–338.
[7] M. Rahmani, J. Mabrouki, B. Regraguy, A. Moufti, M. El'Mrabet, A. Dahchour S. El Hajjaji, Adsorption of (methylene blue) onto natural oil shale: kinetics of adsorption, isotherm and thermodynamic studies, Int. J. Environ. Anal. Chem., (2021) 1–15, doi: 10.1080/03067319.2021.1957466.
[8] S. Ichchoa, E. Khouya, S. Fakhi, M. Ezzine, H. Hannache, R. Pallier, R. Naslain, Influence of the experimental conditions on porosity and structure of adsorbents elaborated from Moroccan oil shale of Timahdit by chemical activation, J. Hazard. Mater., 118 (2005) 45–51.
[9] F.Z. Choumane, B. Benguella, Removal of acetamiprid from aqueous solutions with low-cost sorbents, Desal. Water Treat., 57 (2014) 1–12.
[10] K. Azoulay, I. Bencheikh, J. Mabrouki, N. Samghouli, A. Moufti, A. Dahchour, S. El Hajjaji, Adsorption mechanisms of azo dyes binary mixture onto different raw palm wastes, Int. J. Environ. Anal. Chem., (2021) 1–20, doi: 10.1080/03067319.2021.1878165.
[11] N. Bouzaouit, C. Bidjou-Haiour, Response surface methodological study of glucose laurate, synthesis catalyzed by immobilized lipase from *Candida cylindracea*, Biol. Forum Int. J., 8 (2016) 420–427.
[12] A. Abourriche, A. Adil, M. Oumam, H. Hannache, R. Pailler, R. Naslain, M. Birot, J.-P. Pillot, New pitches with very significant maturation degree obtained by supercritical extraction of Moroccan oil shale, J. Supercrit. Fluids, 47 (2008) 195–199.
[13] H. Ouasif, S. Yousfi, M.L. Bouamrani, M. El Kouali, S. Benmokhtar, M. Talbi, Removal of a cationic dye from wastewater by adsorption onto natural adsorbents, J. Mater. Environ. Sci., 4 (2013) 1–10.
[14] S. Bhowmik, V. Chakraborty, P. Das, Batch adsorption of indigo carmine on activated carbon prepared from sawdust: a comparative study and optimization of operating conditions using response surface methodology, Results Surf. Interfaces, 3 (2021) 100011, doi: 10.1016/j.rsurfi.2021.100011.
[15] Y.C. Sharma, Uma, S.N. Upadhyay, Removal of a cationic dye from wastewaters by adsorption on activated carbon developed from coconut coir, Energy Fuels, 23 (2009) 2983–2988.
[16] A. Zuorro, M. Fidaleo, R. Lavecchia, Response surface methodology (RSM) analysis of photodegradation of sulfonated diazo dye Reactive Green 19 by UV/H_2O_2 process, J. Environ. Manage., 127 (2013) 28–35.
[17] J. Mabrouki, A. Moufti, I. Bencheikh, K. Azoulay, Y. El Hamdouni, S. El Hajjaji, Optimization of the Coagulant Flocculation Process for Treatment of Leachate of the Controlled Discharge of the City Mohammedia (Morocco), International Conference on Advanced Intelligent Systems for Sustainable Development, Springer, Cham, 2019, pp. 200–212.
[18] J. Dasgupta, M. Singh, J. Sikder, V. Padarthi, S. Chakraborty, S. Curcio, Response surface-optimized removal of Reactive Red 120 dye from its aqueous solutions using polyethyleneimine enhanced ultrafiltration, Ecotoxicol. Environ. Saf., 121 (2015) 271–278.
[19] A. Ayach, S. Fakhi, Z. Faiz, A. Bouih, O. Ait malek, A. Benkdad, M. Benmansour, A. Laissaoui, M. Adjour, Y. Elbatal, I. Vioque, G. Manjon, Adsorption of Methylene Blue on bituminous schists from Tarfaya-Boujdour, Chem. Int., 3 (2017) 34.

[20] N. Naowanat, N. Thouchprasitchai, S. Pongstabodee, Adsorption of emulsified oil from metalworking fluid on activated bleaching earth-chitosan-SDS composites: optimization, kinetics, isotherms, J. Environ. Manage., 169 (2016) 103–115.
[21] V.K. Gupta, A. Rastogi, A. Nayak, Adsorption studies on the removal of hexavalent chromium from aqueous solution using a low-cost fertilizer industry waste material, J. Colloid Interface Sci., 342 (2010) 135–141.
[22] O. Sakin Omer, M.A. Hussein, B.H.M. Hussein, A. Mgaidi, Adsorption thermodynamics of cationic dyes (methylene blue and crystal violet) to a natural clay mineral from aqueous solution between 293.15 and 323.15 K, Arabian J. Chem., 11 (2018) 615–623.
[23] R. Ahmad, R. Kumar, S. Haseeb, Adsorption of Cu^{2+} from aqueous solution onto iron oxide coated eggshell powder: evaluation of equilibrium, isotherms, kinetics, and regeneration capacity, Arabian J. Chem., 5 (2012) 353–359.
[24] I. Bencheikh, K. Azoulay, J. Mabrouki, S. El Hajjaji, A. Moufti, N. Labjar, The use and the performance of chemically treated artichoke leaves for textile industrial effluents treatment, Chem. Data Collect., 31 (2021) 100597, doi: 10.1016/j.cdc.2020.100597.
[25] C. Cojocaru, G. Zakrzewska-Trznadel, A. Jaworska, Removal of cobalt ions from aqueous solutions by polymer assisted ultrafiltration using experimental design approach. Part 1: optimization of complexation conditions, J. Hazard. Mater., 169 (2009) 599–609.
[26] N. Abd Malek Nurul, A.H. Jawad, I. Khudzir, R. Razuan, Z.A. AlOthman, Fly ash modified magnetic chitosan-polyvinyl alcohol blend for reactive orange 16 dye removal: adsorption parametric optimization, Int. J. Biol. Macromol., 189 (2021) 464–476.
[27] S. Rahdar, K. Pal, L. Mohammadi, A. Rahdar, Y. Goharniya, S. Samani, G.Z. Kyzas, Response surface methodology for the removal of nitrate ions by adsorption onto copper oxide nanoparticles, J. Mol. Struct., 1231 (2020) 1–10, doi: 10.1016/j.molstruc.2020.129686.
[28] S. Farooq, A. Saeed, M. Sharif, H. Javid, F. Mabood, M. Iftekhar, Process optimization studies of crystal violet dye adsorption onto novel, mixed metal $Ni_{0.5}Co_{0.5}Fe_2O_4$ ferrospinel nanoparticles using factorial design, J. Water Process. Eng., 16 (2017) 132–141.
[29] J.W. Turkey, Exploratory Data Analysis, Addison-Wesley Pub. Co., Reading, MA, 1977.
[30] G.E.P. Box, D.R. Cox, An analysis of transformations, J. R. Stat. Soc., 262 (1964) 11–252.
[31] J. Dasgupta, A. Singh, S. Kumar, J. Sikder, S. Chakraborthy, S. Curcio, H.A. Arafat, Poly(sodium-4-styrenesulfonate) assisted ultrafiltration for methylene blue dye removal from simulated wastewater: optimization using response surface methodology, J. Environ. Chem. Eng., 4 (2016) 2008–2022.
[32] S. Chakraborty, J. Dasgupta, U. Farooq, J. Sikder, E. Drioli, S. Curcio, Experimental analysis, modeling, and optimization of chromium(VI) removal from aqueous solutions by polymer-enhanced ultrafiltration, J. Membr. Sci., 456 (2014) 139–154.
[33] M. Fadil, A. Farah and, B. Ihssane, T. Haloui, Optimization of parameters influencing the hydrodistillation of *Rosmarinus officinalis* L. by response surface methodology, J. Mater. Environ. Sci., 6 (2015) 2346–2357.
[34] S. Jerold, S. Chelladurai, K. Murugan, A.P. Ray, M. Upadhyaya, V. Narasimharaj, S. Gnanasekaran, Optimization of process parameters using response surface methodology: review, Mater. Today: Proc., 37 (2021) 1301–1304, doi: 10.1016/j.matpr.2020.06.466.
[35] M. Feinberg, Validation des Méthodes D'analyse, une Approche de L'assurance Qualité au Laboratoire, Dunod, Paris, 2004.
[36] A. Bennani Karim, B. Mounir, M. Hachkar, M. Bakasse, A. Yaacoubi, Removal of basic dye "Methylene Blue" in aqueous solution by Safi clay, Rev. Sci. L'Eau, 23 (2010) 375–388.
[37] J. Mabrouki, M. Benbouzid, D. Dhiba, S. El Hajjaji, Simulation of wastewater treatment processes with Bioreactor Membrane Reactor (MBR) treatment versus conventional the adsorbent layer-based filtration system (LAFS), J. Environ. Anal. Chem., (2020) 1–11, doi: 10.1080/03067319.2020.1828394.
[38] L. El Fakir, M. Flayou, A. Dahchour, S. Sebbahi, F. Kifani-Sahban, S. El Hajjaji, Adsorptive removal of copper(II) from aqueou solutions on phosphates: equilibrium, kinetics, and thermodynamics, Desal. Water Treat., 57 (2016) 17118–17127, doi: 10.1080/19443994.2015.1112840.
[39] A.A. Azzaz, S. Jellali, H. Akrout, A.A. Assadi, L. Bousselmi, Optimization of a cationic dye removal by a chemically modified agriculture by-product using response surface methodology: biomasses characterization and adsorption properties, J. Environ. Sci. Pollut. Res., 24 (2017) 9831–9846, doi: 10.1007/s11356-016-7698-6.
[40] K. Azoulay, I. Bencheikh, A. Moufti, A. Dahchour, J. Mabrouki, S. El Hajjaji, Comparative study between static and dynamic adsorption efficiency of dyes by the mixture of palm waste using the central composite design, Chem. Data Collect., 27 (2020) 100385, doi: 10.1016/j.cdc.2020.100385.
[41] E. Rachid, T. Mohamed, M. Ahmed, H. Tounsadi, Box-Behnken experimental design for the optimization of methylene blue adsorption onto Aleppo pine cones, J. Mater. Environ. Sci., 6 (2017) 2184–2191.
[42] S. Babel, T.A. Kurniawan, Cr(VI) removal from synthetic wastewater using coconut shell charcoal and commercial activated carbon modified with oxidizing agents and/or chitosan, Chemosphere, 54 (2004) 951–967.
[43] S. Hajati, M. Ghaedi, H. Mazaheri, Removal of methylene blue from aqueous solution by walnut carbon: optimization using response surface methodology, Desal. Water Treat., 57 (2016) 3179–3193, doi: 10.1080/19443994.2014.981217
[44] H.V. Tran, L.T. Hoang, C.D. Huynh, An investigation on kinetic and thermodynamic parameters of methylene blue adsorption onto graphene-based nanocomposite, Chem. Phys., 535 (2020) 110793, doi: 10.1016/j.chemphys.2020.110793.
[45] H. Ouasif, S. Yousfi, M.L. Bouamrani, M. Talbi T. Aïnane, M. El Kouali, Comparative study of adsorption of methylene blue in two natural materials, Phys. Chem. News, 58 (2011) 1–5.
[46] A.A. Azzaz, S. Jellali, A.A. Assadi, L. Bousselmi, Chemical treatment of orange tree sawdust for a cationic dye enhancement removal from aqueous solutions: kinetic, equilibrium and thermodynamic studies, Desal. Water Treat., 57 (2016) 22107–22119.
[47] Q. Xu, T. Liu, L. Li, B. Liu, X. Wang, S. Zhang, L. Li, B. Wang, A.R. Zimmerman, B. Gao, Hydrothermal carbonization of distillers grains with clay minerals for enhanced adsorption of phosphate and methylene blue, Bioresour. Technol., 340 (2021) 125725, doi: 10.1016/j.biortech.2021.125725.
[48] S. Hajati, M. Ghaedi, B. Barazesh, F. Karimi, R. Sahraei, A. Daneshfar, A. Asghari, Application of high order derivative spectrophotometry to resolve the spectra overlap between BG and MB for the simultaneous determination of them: ruthenium nanoparticle loaded activated, carbon as adsorbent, J. Ind. Eng. Chem., 20 (2014) 2421–2427.
[49] A. Ayach, S. Fakhi, Z. Faiz, A. Bouih, O. Ait malek, A. Benkdad, M. Benmansour, A. Laissaoui, M. Adjour, Y. Elbatal, I. Vioque, G. Manjon, Adsorption of Methylene Blue on bituminous schists from Tarfaya-Boujdour, Chem. Int., 3 (2017) 343–352.